Thickness dependent binary behavior of elongated single-domain cobalt nanostructures

S. Evoy,[a] D. W. Carr, L. Sekaric, Y. Suzuki, J. M. Parpia, and H. G. Craighead
Cornell Center for Materials Research and Cornell Nanofabrication Facility, Cornell University, Ithaca, New York 14853

(Received 28 June 1999; accepted for publication 24 September 1999)

We have studied the switching behavior of single-domain cobalt nanostructures using a combination of magnetometry and magnetic force microscopy. The elongated nanostructures are 80×140 nm wide, and range in thickness from 14 to 30 nm. Structures thinner than 20 nm form a single-domain binary system featuring two preferred orientations of the magnetization. An additional double-domain configuration becomes increasingly favorable as the thickness approaches 30 nm. The onset of this double-domain state agrees with previously reported numerical calculations. We also present a quantitative study of interparticle coupling in tightly packed arrays. The local dipolar field increases the squareness of the hysteresis loop as the interparticle separation decreases below 400 nm. © *2000 American Institute of Physics.* [S0021-8979(00)04901-X]

I. INTRODUCTION

The fabrication and characterization of single-domain ferromagnetic nanostructures has been of growing interest from both basic physics and technological standpoints.[1–4] Anisotropic single-domain nanostructures offer a binary system in which data can be stored through the direction of the magnetization along the easy axis.[3,4] Arrays of such individually addressable binary devices could represent a two order of magnitude increase in storage density over conventional media.[4] Several studies have addressed the impact of shape and crystalline anisotropy on the magnetic behavior of microstructured materials.[1,2,4–16] For example, submicron structures exhibit interesting dimension-dependent arrangements of their domain configuration.[4,6,12] Furthermore, the transition from multidomain to single domain was reported in polycrystalline cobalt as lateral dimensions decreased from 200×400 to 150×200 nm.[5] Other studies have also reported evidence of dipolar interaction in arrays of particles.[1,17,18]

A single-domain structure does not necessarily equate to a binary system if other energetically favorable configurations are also available. In this article, we therefore consider magnetic nanostructures in terms of their binary versus nonbinary nature. We have studied the thickness-dependent switching behavior of cobalt nanostructures, and have observed a departure from binary behavior as the thickness approaches 30 nm. We will also present a quantitative study of interparticle interaction effects in tightly packed arrays.

II. EXPERIMENT

Cobalt nanostructures were fabricated using electron beam lithography, metal evaporation, and liftoff. A 160 nm thick resist bilayer is produced on a silicon wafer by the successive spinning and curing of 496 and 950 K molecular weight polymethylmetacrylate (PMMA). This bilayer enhances the undercut of the resist, insuring a clean liftoff of the metal structures. The wafer is exposed in a Leica VB6 lithography system using a $V=30$ kV ($I=5$ nA) beam. An optimal dose of 1400 μC/cm^2 is found under these conditions. After development of the PMMA, cobalt is electron beam evaporated at a rate of 1 nm/s. No adhesion layer is used. Immersion in a sonicated 1:1 mixture of acetone/methylene chloride lifts off the unexposed resist. The structures are expected to be polycrystalline under these deposition conditions.

Structures are designed as rectangles 80×140 nm in size. The thickness is varied from $t=14$ to 30 nm (as measured from atomic force microscopy profiles). Unless otherwise noted, the particles are written on a 60° triangular lattice with center-to-center spacings ranging from $s=150$ to 700 nm. The dimensions of the resulting structures deviate by only a few nanometers from the design parameters, and their corners show significant rounding (Fig. 1).

Magnetic force microscopy (MFM) is performed using a Digital Instruments Dimension 3000 microscope with standard magnetic force etched silicon probes. Magnetic information is recorded in ambient through the acquisition of tapping mode phase information. Approximating the tip by a small magnetic dipole, the tip–sample interaction induces a phase shift proportional to $\delta^2 H_z/\delta z^2$, where H_z is the out-of-plane component of the local field.[19] A separation of 30 nm is kept between tip and sample during magnetic recording by using the software-integrated Lift Mode™. Samples are magnetized *ex situ* in a solenoid prior to imaging. Magnetization curves are acquired at 298 K in a Quantum Design superconducting quantum interference device (SQUID) magnetometer. While MFM imaging was performed on 30×30 μm arrays, signal-to-noise considerations required the fabrication of 2.5×2.5 mm arrays for the acquisition of SQUID magnetization curves.

[a]Electronic mail: se20@cornell.edu

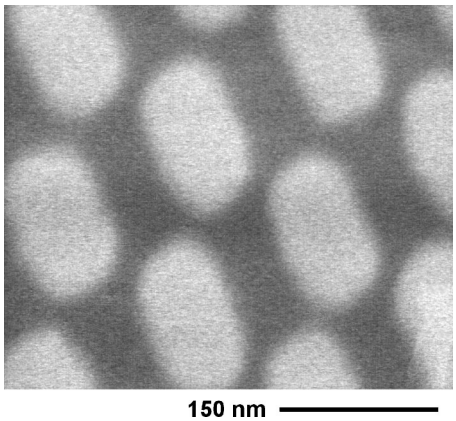

FIG. 1. Scanning electron micrograph of a tightly packed array of 80 $\times 140 \times 20$ nm cobalt nanostructures on a $s = 150$ nm triangular lattice.

III. RESULTS AND DISCUSSION

A. MFM versus SQUID

Figure 2 shows a typical MFM image of a square array of $80 \times 140 \times 30$ nm nanostructures. Bright and dark areas correspond to the magnetic field lines emerging from and merging into the sample, respectively. The well-known[5,7,17] contiguous bright/dark pair indicative of single-domain magnetization characterizes several structures. It specifically corresponds to field lines curving out from one pole and into the opposite pole, respectively. However, as pointed out in Ref. 3, the polycrystalline nature of the structures prevents the formation of a true single domain. The term single domain is better described in this context as an almost uniform configuration in which the individual grains tend to align their magnetization along a same direction.[3]

Other particles manifest a more complex structure suggestive of a different configuration. This configuration becomes more prevalent as the thickness increases above 20 nm. Its magnetic signature is characteristic of the formation of a single-domain wall.[12] Numerical modeling of square Permalloy single-domain elements has shown that a closed vortex configuration is energetically favorable over more uniform configurations as the thickness is increased.[11] It is not surprising that we observe the formation of a domain wall rather than a closed vortex considering the elongated nature of our structures.

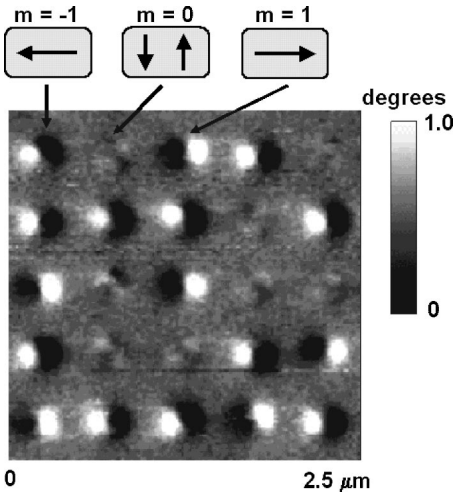

FIG. 2. Typical MFM image of $80 \times 140 \times 30$ nm cobalt nanostructures on a widely spaced ($s = 500$ nm) square lattice.

A visual inspection of MFM images can be used to generate a semiquantitative magnetization curve.[16,17] As described at the top of Fig. 2, we assign a value of reduced magnetization $m = -1, 0, +1$ to each state. The sample is initially fully magnetized in the $m = -1$ state in a field of $B \sim -1200$ G [Fig. 3(a)]. The array is then successively imaged following the application of an increasing switching field [Figs. 3(b) and 3(c)]. An average $\bar{m}$ is computed from the inspection of 400–500 particles for each data point. Given that the field is not sustained during imaging, a sequence of such images provides a semiquantitative graph of the remanent magnetization of the sample.[16,17]

Figure 4 shows the result of this process for widely spaced ($s = 600$ nm) $80 \times 140 \times 18$ nm particles written on a triangular lattice. Figure 4 also displays the corresponding hysteresis curve acquired with the SQUID. The SQUID hysteresis and the MFM-acquired data both show an onset at $B = 400$ G and a similar slope in the $B = 400 - 800$ G range. As expected from single-domain structures, the similarity suggests that the switching distribution of the individual binary particles governs the hysteresis slope of the array.[16] This consistency allows the combination of the quantitative information of the SQUID with the qualitative spatial resolution of the MFM.

The SQUID hysteresis curve also features a substantial kink in the $B = 0 - 400$ G range that is absent from the MFM-acquired data. One could erroneously argue that the MFM overlooks the kink due the binary nature of the computational approach. However, while the SQUID hysteresis is acquired under a sustained field, the MFM images are acquired after the field has been returned to zero. In addition, the configuration and intensity of the magnetic spatial signature remain unchanged after exposure to these low fields. These observations therefore rather suggest some reversible rearrangement at lower fields, possibly through the formation of minor vortices, domain wall, or coherent rotation. The particles will return to their fully magnetized equilibrium state if the field is removed without reaching the switching threshold. The reversibility of the phenomenon would suppress the kink in the MFM-acquired remanent information. This picture is schematically represented at the bottom of Fig. 4.

B. Thickness dependence

The experiment described above has been repeated for several particle thicknesses. All samples are initially magnetized in a $B = -1200$ G field. Figure 5 shows MFM images of the remanent magnetization of particles of increasing thickness (rows) after exposure to an increasing switching field (columns). All particles initially show a single-domain $m = -1$ magnetization (first column of Fig. 5). After exposure to intermediate switching fields ($B \sim +100 - 600$ G), some particles show the more complex configuration de-

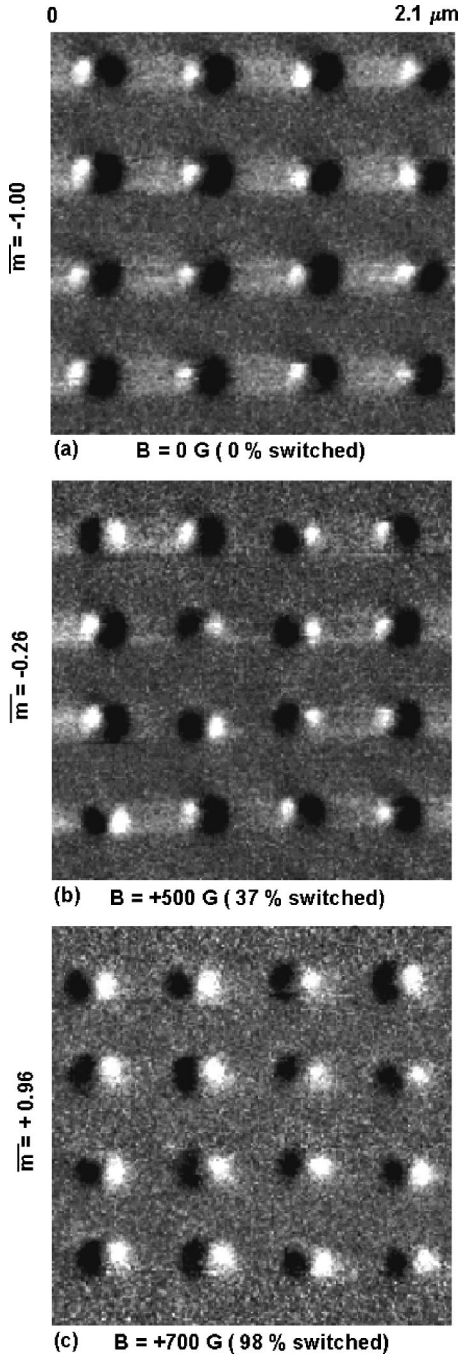

FIG. 3. Sequence of MFM images of 80×140×17 nm cobalt nanostructures on a widely spaced ($s=600$ nm) square lattice. The particles are initially magnetized in the $m=-1$ state by applying a $B=-1200$ G field. Successive images are then taken following an application of an increasing opposite switching field. (a) Image of initial magnetization. (b) After exposure to $B=+500$ G. (c) After exposure to $B=+700$ G. The external field is not sustained during imaging.

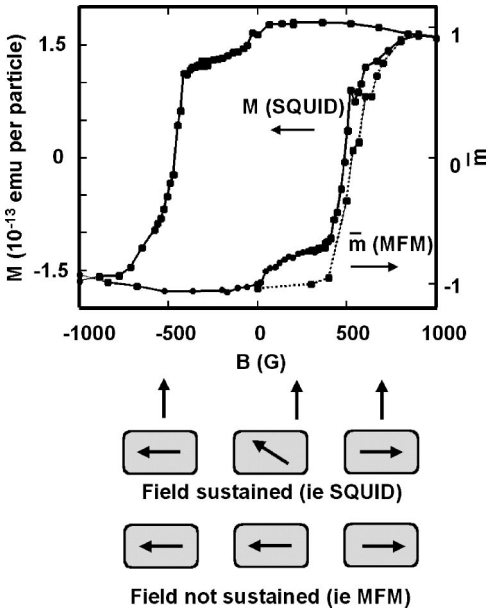

FIG. 4. Magnetization curves acquired with MFM and SQUID on 80×140 nm particles written on a widely spaced triangular lattice. The structures are 17 nm thick for the MFM data and 18 nm thick for the SQUID data. The separation between these noninteracting particles is $s=600$ and 500 nm, respectively. While the external field is sustained during the SQUID acquisition, MFM data are acquired after it is returned to zero. Bottom: Schematic explanation of the features seen in the curves. Under a sustained field, particles first undergo some reversible rearrangement of their magnetization until a permanent switching threshold is reached. Particles return to their original configuration if the external field is removed without reaching threshold.

scribed in Sec. III A (second column). This re-emerging double-domain state remains stable even if the field is removed, and its occurrence increases with thickness. By further increasing the field, all particles switch again to the opposite fully magnetized $m=1$ configuration (third column). Assigned to a reduced magnetization value of $m=0$, the stable remanent double-domain state reappearing in thicker particles at lower fields translates to an earlier onset of the corresponding MFM-computed remanent curve [Fig. 6(a)].

This thickness-dependent behavior also appears in the corresponding SQUID hysteresis curves [Fig. 6(b)]. The slope of the hysteresis in the low-field 0–400 G region increases as the thickness increases from $t=14$ to 24 nm, and culminates in the sudden appearance of a distinctively abrupt slope in this low range for the 30 nm thick particles. An additional unknown material could alternatively explain this additional feature. However, the thickness at which it appears and its relative importance agree well with the MFM observations of Fig. 5. The abrupt slope observed at low fields for the 30 nm thick structures is therefore most likely caused by the previously described departure from binary behavior.

Cowburn and Welland have numerically calculated the magnetic self-energy of various magnetization configurations in square ferromagnetic nanostructures.[11] Their simulation of 50–100 nm wide square Permalloy particles predicts a thickness dependence of the lowest energy configuration. Specifically, the low-energy state shifts from roughly uniform configurations to a vortex like state when the thickness increases beyond $t=10-20$ nm. The transition is understood as a competition between the reduction of exchange energy in the directed states and the reduction of magnetostatic energy in the vortex.[11] The thickness at which we observe this transition agrees well with the numerical predictions in spite of the elongated shape that promotes a domain wall rather than a closed vortex.

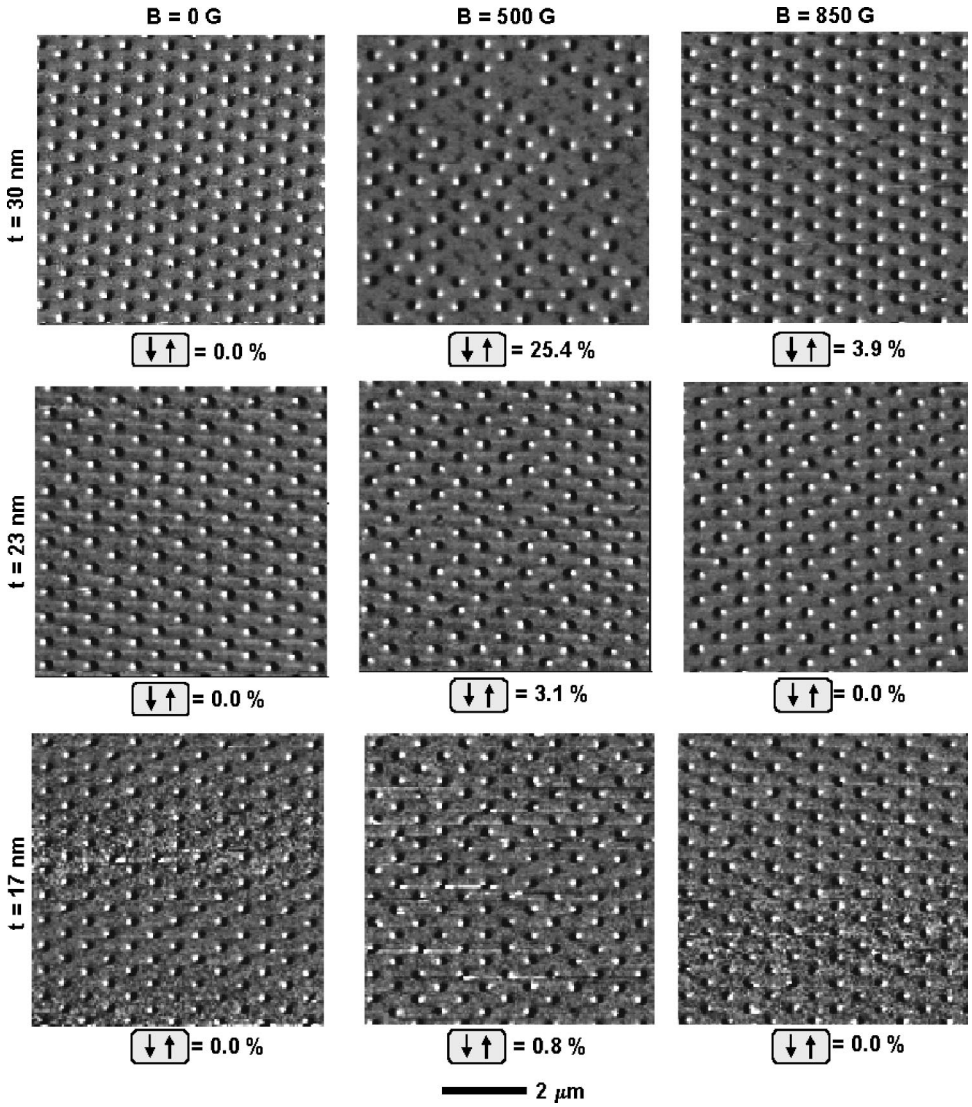

FIG. 5. Sequence of MFM images of 80×140 cobalt nanostructures on a widely spaced ($s=600$ nm) triangular array. The thickness varies from 17 to 30 nm (rows). The particles are initially magnetized in the $m=-1$ state by applying a $B=-1200$ G field. Successive images are then taken following an application of an increasing opposite switching field (columns). The percentage of particles in a double-domain state appears at the bottom of each image.

Finally, the thickness dependence of the saturation magnetization can also be extracted from Fig. 6(b). Assuming straight sidewalls, we would expect the saturation value to scale with thickness. The data do present a rough linear relationship, but also feature a nonzero intercept with the origin. The presence of several nanometers of oxide on the cobalt surface, a departure from the straight sidewall assumption, or a grain size-related lack of thickness uniformity in thinner particles could explain this nonzero intercept.

In summary, all particles can be forced into a fully magnetized $m=\pm1$ configuration. A reversible rearrangement occurs in thinner particles until a permanent switching threshold is reached. The formation of a stable domain wall becomes increasingly favorable as particle thickness is increased. Thinner particles therefore form a binary system in which permanent switching directly occurs to the opposite fully magnetized direction. On the other hand, thicker particles form a quaternary rather than a binary system in which intermediate $m=0$ remanent states are also available. The thickness-dependent onset of this additional state is in approximate agreement with the numerical calculations reported in Ref. 11.

C. Separation dependence

All results presented up to this point were obtained on widely spaced arrays ($s=600$ nm) of noninteracting particles. Evidence of interparticle dipolar interaction has previously been reported for $1000\times100\times50$ nm Permalloy structures.[17] Here in Sec. III C, we present additional quantitative evidence of this interaction in the switching behavior of substantially smaller single-domain cobalt particles.

Figures 4 and 6 showed that an external field of $B=650$ G was sufficient to switch a majority of noninteracting particles. We expect the local dipolar field from the majority to inhibit or promote the switching of the ensemble.[17,18] Analogous to the behavior of Permalloy,[17] our MFM images indeed reveal the tendency of neighboring particles to switch collectively as their separation decreases. At higher fields, the local field from this switched majority promotes the switching of the rogue minority that otherwise would not have switched, resulting in an increase of the switching probability at a given switching field [Fig. 7(a)]. Conversely, at lower fields, the unswitched majority inhibits the switching of the minority that otherwise would have switched. The net

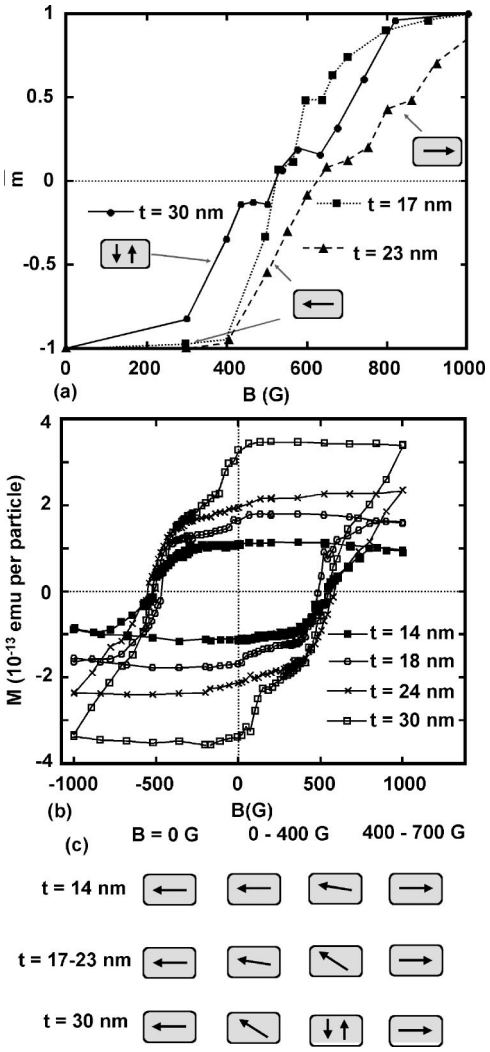

FIG. 6. (a) MFM switching curves for the experiment described in Fig. 5. (b) SQUID hystersis curves of particles with a similar range of thickness. The separations between these noninteracting particles are $s=600$ and 500 nm for (a) and (b), respectively. Both approaches reveal an early onset of the switching for the 30 nm thick structures. This thickness corresponds to the appearance of the double-domain configuration seen in Fig. 5. Bottom: Schematic description of the phenomenon. Thinner particles form a binary system, and will directly switch from one magnetized state to the opposite magnetized state. Thicker particles will first undergo an intermediate transition in a double-domain state before switching again to the opposite direction.

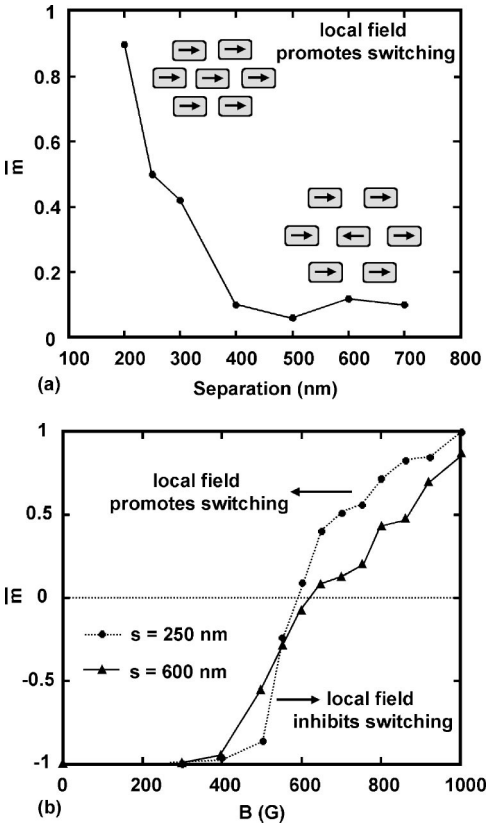

FIG. 7. (a) Switching of structures under a same external field ($B=+650$ G) at varying spacings. The switched majority promotes the switching of rogue particles, resulting in an increase of the switching probability as the array becomes tighter. (b) MFM switching curves for widely and tightly packed arrays ($s=600$ and 250 nm, respectively). The local dipolar field slightly increases the slope of the switching curve in tightly packed arrays.

result is an increase of the switching slope as the separation is decreased below 400 nm [Fig. 7(b)]. This cascade effect is also seen in the SQUID magnetization curves (Fig. 8) as an increase of the squareness of the hysteresis loop.

Dipolar interaction is to be avoided in quantum storage applications since it may compromise the reliability and stability of the individual bits. Onset of interaction for spacings under 400 nm would represent a density limit of ~ 5 Gb/in^2, on the order of magnitude of already existing technologies. Alternative geometries such as imbedded out-of-plane elongated structures[4] may partially address the issue by decreasing their lateral extent for a same particle volume. Furthermore, the spatial extent of such interactions is likely to decrease with decreasing particle volume at the expense of signal to noise. Further parameter-dependent systematic studies of this interaction would therefore provide important additional technological and physical insights.

IV. CONCLUSIONS

We have reported a study of the magnetization behavior of cobalt nanostructures using a combination of magnetic force microscopy and SQUID magnetometry. We have par-

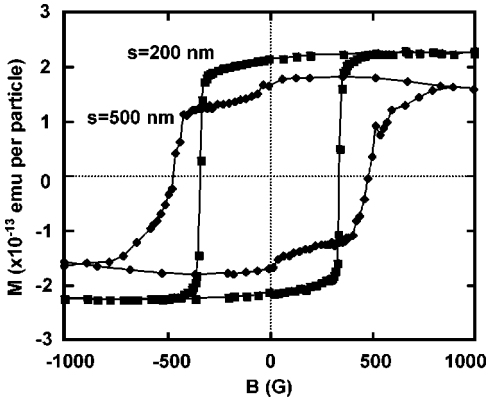

FIG. 8. SQUID hystersis curves for widely and tightly packed arrays ($s=500$ and 200 nm, respectively). As observed with MFM (Fig. 7), the local dipolar field in tightly packed arrays increased the switching slope of the entire array, resulting in an increase of the squareness of the hysteresis.

ticularly investigated the binary nature of the system, and documented the onset of an additional remanent state as the particle thickness exceeds 20 nm. Even though the particles could still be magnetized as single domain, the presence of additional energetically favorable states represents a departure from a true ''binary'' system that is desired in quantum storage applications.

We have also presented additional quantitative evidence on the effect of local fields in tightly packed arrays. As spacing decreases below $s = 400\,\text{nm}$, the interparticle coupling increases the slope of the switching curve, resulting in an increase of squareness of the hysteresis of the entire array. Such interaction is of importance for the technological implementation of these devices.

ACKNOWLEDGMENTS

This work was supported by the National Science Foundation through the Cornell Center of Materials Research and the Cornell Nanofabrication Facility (CNF). Fabrication of nanostructures was performed at the CNF. The authors wish to thank Dr. Vincent Balbarin for his assistance with the SQUID magnetometer and for several insightful discussions.

[1] J. F. Smyth, S. Schultz, D. Kern, H. Schmid, and D. Yee, J. Appl. Phys. **63**, 4237 (1988).
[2] J. F. Smyth, S. Schultz, D. R. Fredkin, D. P. Kern, S. A. Rishton, H. Schmid, M. Cali, and T. R. Koehler, J. Appl. Phys. **69**, 5262 (1991).
[3] R. M. H. New, R. F. W. Pease, and R. L. White, J. Vac. Sci. Technol. B **12**, 3196 (1994).
[4] S. Y. Chou, M. Wei, P. R. Krauss, and P. B. Fischer, J. Vac. Sci. Technol. B **12**, 3639 (1994); J. Appl. Phys. **76**, 6673 (1994); J. Vac. Sci. Technol. B **12**, 3695 (1994); S. Y. Chou, P. R. Krauss, and L. Kong, J. Appl. Phys. **79**, 6101 (1996); B. Cui, W. Wu, L. Kong, X. Sun, and S. Y. Chou, *ibid.* **85**, 5534 (1999).
[5] R. M. H. New, R. F. W. Pease, R. L. White, R. M. Osgood, and K. Babcock, J. Appl. Phys. **79**, 5851 (1996); R. M. H. New, R. F. W. Pease, and R. L. White, J. Magn. Magn. Mater. **155**, 140 (1996); J. Vac. Sci. Technol. B **13**, 1089 (1995).
[6] M. Hehn, K. Ounadjela, J.-P. Bucher, F. Rousseaux, D. Decanini, B. Bartenlian, and C. Chappert, Science **272**, 1782 (1996); H. Hehn, K. Ounadjela, R. Ferre, W. Grange, and F. Rousseaux, Appl. Phys. Lett. **71**, 2833 (1996); R. Ferre, Comput. Mater. Sci. **10**, 205 (1998).
[7] G. Meier, M. Kleiber, D. Grundler, D. Heitman, and R. Wiesendanger, Appl. Phys. Lett. **72**, 2168 (1998); R. Wiesendanger, M. Bode, M. Kleiber, M. Lohndorf, R. Pascal, A. Wadas, and D. Weiss, J. Vac. Sci. Technol. B **15**, 1330 (1997).
[8] M. Grimsditch, Y. Jaccard, and I. K. Schuller, Phys. Rev. B **58**, 11539 (1998).
[9] J. Areas, A. Hernando, J. M. Barandiaran, C. Prados, M. Vazquez, P. Marin, and A. Neuweiler, Phys. Rev. B **58**, 5193 (1998).
[10] J. I. Martin, J. Nogues, I. K. Schuller, M. J. Van Bael, K. Temst, C. Van Haesendonck, V. V. Moshchalkov, and Y. Bruynseraede, Appl. Phys. Lett. **72**, 255 (1998).
[11] R. P. Cowburn and M. E. Welland, Appl. Phys. Lett. **72**, 2041 (1998); Phys. Rev. B **58**, 9217 (1998).
[12] E. F. Wassermann, M. Thielen, S. Kirsch, A. Pollmann, H. Weinforth, and A. Carl, J. Appl. Phys. **83**, 1753 (1998).
[13] K. J. Kirk, J. N Chapman, and C. D. W. Wilkinson, Appl. Phys. Lett. **71**, 539 (1997); M. Ruhrig, B. Khamsehpour, K. J. Kirk, J. N. Chapman, P. Aitchison, S. McVittie, and C. D. Wilkinson, IEEE Trans. Magn. **32**, 4452 (1996).
[14] S. Wirth, M. Field, D. D. Awschalom, and S. von Molnar, Phys. Rev. B **57**, R14028 (1998).
[15] D. R. Fredkin and T. R. Koehler, J. Appl. Phys. **67**, 5544 (1990); D. R. Fredkin, T. R. Koehler, J. F. Smyth, and S. Schultz, *ibid.* **69**, 5276 (1991); P. H. Bryant, J. F. Smyth, S. Schultz, and D. R. Fredkin, Phys. Rev. B **47**, 11255 (1993).
[16] R. D. Gomez, M. C. Shih, R. M. H. New, R. F. W. Pease, and R. L. White, J. Appl. Phys. **80**, 342 (1996).
[17] G. A. Gibson and S. Schultz, J. Appl. Phys. **73**, 4516 (1993).
[18] C. Stamm, F. Marty, A. Vaterlaus, V. Weich, S. Egger, U. Maier, U. Ramsperger, H. Fuhrmann, and D. Pescia, Science **282**, 449 (1998).
[19] D. Rugar, H. J. Mamin, P. Guethner, S. E. Lambert, J. E. Stren, I. McFayden, and T. Yogi, J. Appl. Phys. **68**, 1169 (1990).